

Direct observation of magnetic domains by Kerr microscopy in a Ni-Mn-Ga magnetic shape-memory alloy

O. Perevertov,^{1,*} O. Heczko,¹ and R. Schäfer^{2,3}

¹*Department of Functional Materials, Institute of Physics of the Czech Academy of Sciences, Praha 8, Czech Republic*

²*Leibniz Institute for Solid State and Materials Research (IFW) Dresden, Institute for Metallic Materials, Helmholtzstrasse 20, D-01069 Dresden, Germany*

³*Institute for Materials Science, TU Dresden, 01062 Dresden, Germany*

(Received 13 February 2017; published 27 April 2017)

The magnetic domains in a magnetic shape-memory Ni-Mn-Ga alloy were observed by magneto-optical Kerr microscopy using monochromatic blue LED light. The domains were observed for both single- and multivariant ferroelastic states of modulated martensite. The multivariant state with very fine twins was spontaneously formed after transformation from high-temperature austenite. For both cases, bar domains separated by 180° domain walls were found and their dynamics was studied. A quasidomain model was applied to explain the domains in the multivariant state.

DOI: [10.1103/PhysRevB.95.144431](https://doi.org/10.1103/PhysRevB.95.144431)

I. INTRODUCTION

The Ni-Mn-Ga Heusler alloy exhibits magnetic shape-memory (MSM) phenomena [1–2]. These multiferroic effects originate from a strong coupling between ferroelasticity and ferromagnetism [2–5]. The coupling can result in giant magnetic-field-induced strain up to 12% under applied magnetic field [6–8] and large magnetocaloric effects [9].

The giant strain occurs due to the magnetic-field-induced reorientation of the ferroelastic domains called martensitic twins. These twins form during a phase transformation from a high-temperature cubic phase to a phase with lower symmetry called “martensite” to secure the compatibility between the phases. The twins can also be formed directly in the martensitic phase by deformation. The twins or structural domains with different orientation are separated by twin boundaries. Owing to the strong coupling between magnetization and crystal lattice structure and extremely high mobility of the twin boundaries in Ni-Mn-Ga [10], the twin distribution can be manipulated by moderate magnetic fields. Instead of simple rotation of magnetization, the twin with preferable orientation (or lower Zeeman energy) in the magnetic field grows by twin boundary motion at the expense of the twins with different orientation [1,2,11]. Due to the low lattice symmetry this process results in large field-induced macroscopic deformation.

Apparently, the knowledge of the coupling of the magnetic domain structure with the martensitic twin variants is crucial for understanding and modeling the MSM phenomenon. A number of experimental and theoretical papers were already devoted to the magnetic domain structure in Ni-Mn-Ga alloys: domains were imaged by optical microscopy [12], scanning electron microscopy (SEM) [12–13], magnetic force microscopy (MFM) [14], the Bitter pattern technique [12,15], Lorentz transmission electron microscopy (TEM) [16], electron holography [17], the interference-contrast-colloid (ICC) method [18–19], and using a magneto-optical indicator film (MOIF) based on polarized optical light microscopy [14,19].

Most of these observations were made in static imaging modes at zero external magnetic field. The only technique that has allowed for some real-time observation of magnetization processes so far is optical microscopy using MOIF. This technique, however, suffers from a number of serious limitations as the contrast is indirect as it is caused by stray fields emerging from the MSM specimen. The disadvantages are low spatial resolution as the domains are visible only at low magnification, the domain contrast of the eigendomains of the MOIF garnet film is superimposed in the obtained image at low fields, and above all the indicator film itself can be affected by the same external magnetic field as used to drive the domains.

Magneto-optical Kerr microscopy, on the other hand, is a widely used method for magnetic domain observation and particularly for studying the magnetic domain wall (DW) dynamics, e.g., in iron-based materials, where the magnetic domains can be observed at real time with high resolution and contrast at different scales and speeds [1,20–21]. This method could be very useful for the investigation of domain dynamics and their interaction with differently oriented ferroelastic domains. To date, however, no direct Kerr contrast was observed on Ni-Mn-Ga alloys. The missing magnetic Kerr contrast was discussed many times and ascribed to a vanishing Kerr rotation for Ni-Mn-Ga type material [22].

Recently, however, we demonstrated that an electropolished Ni-Mn-Ga single crystal exhibits a small Kerr rotation in a broad spectral range including visible light both for the high-temperature cubic parent phase called “austenite” and the 10 M martensite state [23]. The measurement showed that the Kerr rotation angle changes sign and crosses zero in the middle of the visible light range [16], which may explain why previous attempts using white light were unsuccessful. The maximum Kerr rotation angle was observed for red (50 millidegrees for 1.65 eV, $\lambda = 750$ nm) and violet light (40 millidegrees for 3.27 eV, $\lambda = 380$ nm). Conventional microscopy lamps provide continuous light spectra (white light). Owing to the changing sign of the Kerr rotation and by considering the wavelength-dependent sensitivity of the detector (the camera in the case of Kerr microscopy), the overall Kerr signal may partly or even completely compensate. By using a blue LED with a peak in the spectrum (at 460 nm

*Author to whom correspondence should be addressed: perevert@fzu.cz

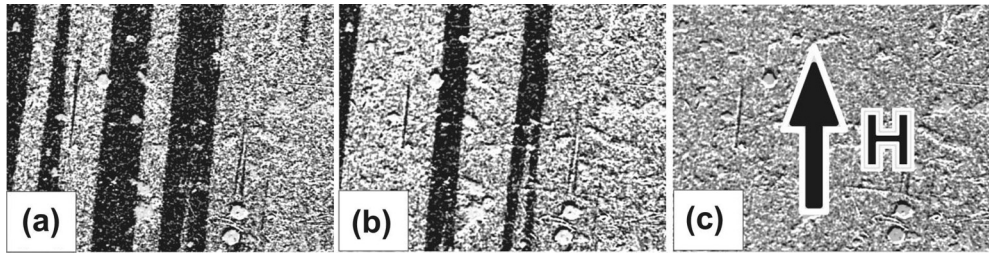


FIG. 1. Magnetic domains in a single-variant state after demagnetization (a) and at applied fields of 10 mT (b) and 17 mT (c). The frame size is $0.65 \times 0.85 \text{ mm}^2$. The applied magnetic field direction is shown in (c).

in our case), however, the compensation of Kerr intensity can be avoided as most of the Kerr signal is generated in a narrow band of wavelength. Here we present a direct Kerr observation of magnetic domains on a $\text{Ni}_{50}\text{Mn}_{28}\text{Ga}_{22}$ single crystal using high-power blue LED illumination in a wide-field Kerr microscope.

II. EXPERIMENTAL

The domain observation was performed on a single-crystalline sample with a nominal composition of $\text{Ni}_{50}\text{Mn}_{28}\text{Ga}_{22}$ in the shape of a flat rectangle with dimensions of $6.7 \times 6.7 \times 1.5 \text{ mm}^3$. The main surface was an approximate (100) plane. A slight misorientation was due to imprecise cutting and particularly a martensitic transformation from a cubic to monoclinic lattice. At room temperature the sample was in the five-layered modulated martensitic state called 10 M. The transformation temperature to austenite was about 310 K. The imaged surface was first carefully mechanically polished and then electropolished in the single-variant state. However, some artifacts due to the presence of spurious variants during polishing appeared on the surface and therefore the whole surface was not perfectly flat. All polishing was done at room temperature.

The arrangement of ferroelastic domains or twin variants on the surface was examined by circular differential interference (Nomarski) contrast and polarization microscopy using an optical Zeiss Axio Imager.Z1m microscope. The surface relief is well visualized by Nomarski contrast, while in polarized light it becomes visible due to some different optical activity of the variants.

For Kerr imaging, a Carl Zeiss microscope of the type AxioScope with a $10 \times /0.25$ objective lens was used. Instead of conventional xenon or mercury lamps; however, the light from high-power blue light emitting diodes (peak wavelength at 460 nm) was used. Finally high contrast difference images were created by digitally subtracting a background image of the saturated state from an acquired image with domains. To avoid the effect of the sample displacement under applied magnetic field, an automatic compensation of the sample motion was used based on piezo actuators.

III. RESULTS AND DISCUSSION

First we consider the simplest case of a single-variant state; i.e., the whole sample is in a single-crystal state with the easy axis of magnetization along the c axis [6]. The single-variant state was obtained by applying a magnetic field of 400 mT

parallel to the [001] direction of one variant. The martensitic lattice orientation is inherited from the austenite [6,11]. After switching off the field, regular 180° domains showed up (Fig. 1). The magnetization in each domain was aligned parallel and antiparallel to the easy c axis and the DWs were perfectly straight. The magnetization process was realized by a simple DW motion with the growth of the domains along the applied field at the expense of opposite ones. Details of this process are shown in videos in the Supplemental Material [24]. Video 1 shows magnetic domains during the magnetization process for a single-variant state, video 2 for a multivariant state.

To obtain a multivariant state, the sample was heated up and then cooled down from the austenite state at 320 K to ambient temperature. As a result, a number of fine twins were spontaneously formed. In Fig. 2 the magnetic domains are shown for the resulting multivariant state together with the background image. At first glance, large domains seemingly separated by 180° DWs are apparent. However, the orientation of these domains is different compared to those of the single-variant state and obviously they do not follow any of the easy axes of the twin variants. So the domain structure seems to be more complex compared to the single-variant state.

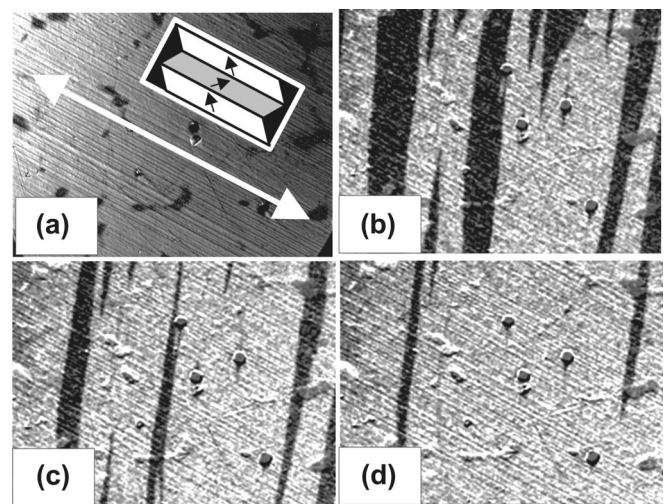


FIG. 2. Background image of fine twins (a) and corresponding magnetic domains for applied fields of 0 mT (b), 8 mT (c), and 13 mT (d). The white arrow in (a) marks the twin boundary plane and the inset schematically shows the martensitic twin microstructure. The applied field direction was approximately vertical. The average size of the twins is about $10 \mu\text{m}$. One frame is $0.65 \times 0.85 \text{ mm}^2$ in size.

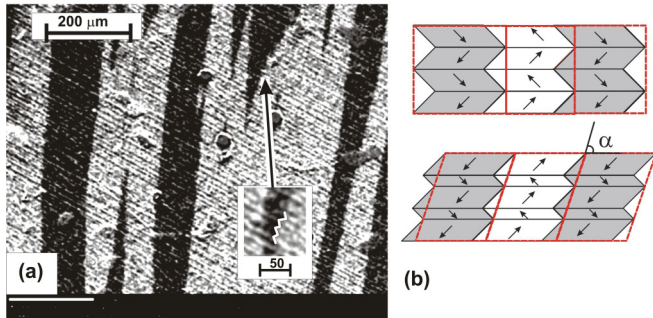


FIG. 3. Magnetic domains of the twinned sample in the demagnetized state (a) together with sketches of the magnetic domain structure for equal (upper image) and nonequal (lower image) volumes of twins with different orientations (b). The inset in (a) shows an enlarged spot where the predicted “stairs” are seen.

To gain deeper insight, the domains in the demagnetized state are shown again in Fig. 3, but now in a magnified version together with sketches of the corresponding magnetization pattern. Such a magnetic microstructure is known from structural studies of similar samples [10]. Owing to the relatively strong uniaxial magnetic anisotropy, the magnetization in each domain follows the easy *c* axis in each variant and the bar domains are separated by 180° domain walls similarly to the single-variant state. At each twin boundary the domains are “reflected” to follow the local easy axis [25]; the horizontal magnetization component thus changes its direction while the vertical component does not [see Fig. 3(b)]. Seen on a larger scale, so-called “quasidomains” [1] are formed that are separated by 180° quasidomain walls. The width of the quasidomains is similar to that in the single-variant state.

In the quasidomains the average magnetization is aligned along quasidomain boundaries while the local magnetization fluctuates from twin to twin. The twin boundaries act at the same time as 90° domain walls since the magnetization changes direction by 90° across the boundaries. In the simplest case of twins having exactly the same width, the observed 180° quasidomain boundaries are aligned perpendicular to the

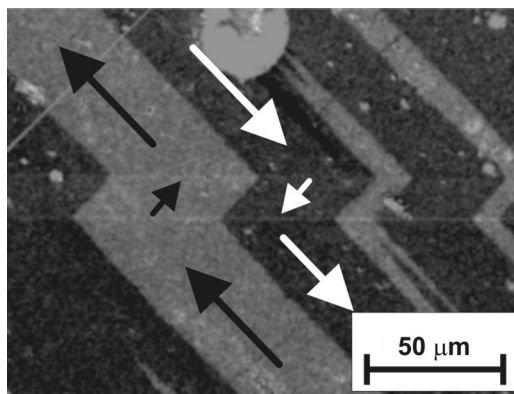


FIG. 4. Detailed view of the magnetic domains of the twin microstructure with only three twins separated by two twin boundaries (weak horizontal lines) in the demagnetized state. The predicted “stairs” are quite apparent. The magnetization direction is shown by arrows.

twin boundaries. If the width of twins is not equal, the local quasidomain boundary direction is given by the ratio of the twin boundary widths in order to form a magnetic-pole-free quasidomain wall orientation. Taking *a* and *b* twin widths and assuming that their ratio is constant, the angle between quasidomain wall orientation and twin boundary is given by

$$\alpha = 135^\circ - \arctan(b/a). \tag{1}$$

The model of the fine twin microstructure presented in Fig. 3(b) implies that the quasidomain boundaries are not straight but rather have a staircase shape. Due to the limited resolution of the Kerr micrographs, the staircase shape is not very apparent for the given magnification. However, a detailed look reveals some spots where “stair” or “teeth” patterns are indeed indicated [inset in Fig. 3(a)]. Clear evidence of the staircase structure is given in Fig. 4 that was obtained at a five times higher magnification compared to Fig. 3. Here three twins are separated by two twin boundaries. The middle twin is much thinner compared to its neighbors. As a consequence, the local quasidomain direction is close to 45° [see Eq. (1)] with respect to the twin boundaries.

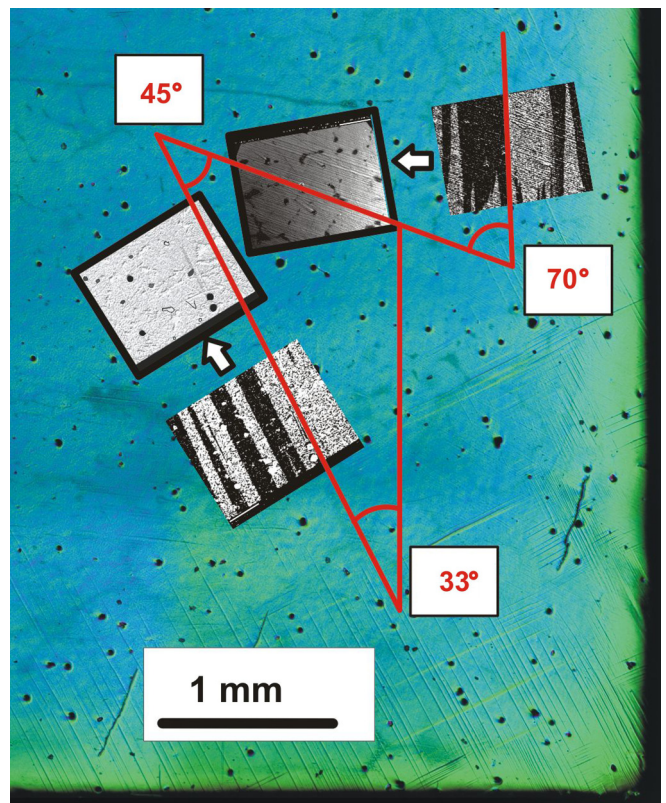


FIG. 5. Optical micrographs of the sample in the cubic austenite state in order to show the position and orientation of the previously presented picture frames (indicated by arrows) in the multivariant state (two right frames) and in the single-variant state (frames on the left). The corresponding magnetic domains are also shown close to the background images. The bottom right corner of the 6.7 × 6.7 mm² sample is shown. The artifacts of residual twins formed during polishing are visible as short diagonal lines. The black spots due to pit corrosion serve as fiducial marks, helping to identify the positions of the picture frames.

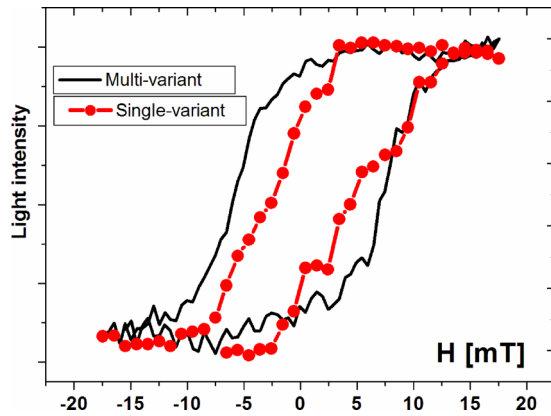


FIG. 6. Kerr hysteresis loops for the multi- and single-variant states, obtained by integrating the Kerr contrast in the microscope and plotting it as a function of magnetic field.

Apart from their intrinsic staircase structure, the quasidomains behave in the same way as regular 180° domains in a uniaxial single crystal. By application of a field the magnetization changes by a simple quasidomain boundary motion as shown in Fig. 2. Again, details of the magnetization process are shown in video 2 in the Supplemental Material [24]. The quasidomain boundaries disappear at the saturation field of about 20 mT. This field was below the critical value for twin boundaries so that the underlining twin microstructure did not change during the whole magnetization process. To move the twin boundaries a field of at least 100 mT is usually needed [13,25].

The localization of the spots where the domain images of the single- and multivariant states were taken is shown in Fig. 5. The magnetic domain observations were done several millimeters away from the sample edges close to the center in order to reduce the demagnetization effect. One of the two possible easy magnetization axes in the single-variant state has an angle of 33° with respect to the vertical axis in Fig. 5. The twin boundaries of the finely twinned sample are at 45° with respect to both easy c axes of each twin variant. The observed quasidomains are at 70° with respect to twin boundaries due

to averaging in the finely twinned microstructure. From the angle together with Eq. (1) we can estimate the local twin distribution with an average ratio of the twin widths with different orientation to be about 2:1.

Surface-sensitive Kerr hysteresis loops for both states are shown in Fig. 6. The coercivity determined from the Kerr loop was about 6–7 mT in the single-variant state, which is similar to the value that was obtained for the whole sample by a vibrating sample magnetometer. The coercivity of the multivariant state was nearly twice as large indicating the pinning of domain walls on the twin boundaries.

IV. CONCLUSIONS

In conclusion, we have observed the magnetic domains in a Ni-Mn-Ga single crystal in the martensitic state by *direct* magneto-optical Kerr microscopy. By using blue light we were able to observe the magnetic domains both in the single- and multivariant twin microstructure in all relevant details. In both cases the observed domains appeared as bar domains separated by 180° DWs. However, in the multivariant state they actually showed up as “quasidomains” having a fine magnetic domain substructure inside the twins or ferroelastic domains. In these domains the real 180° domains follow the local easy c axis and are reflected at each twin boundary. At the same time the twin boundaries represented nearly 90° magnetic domain walls. We revealed the dynamics of the magnetic domains and quasidomains by measuring the full magnetization cycle. The observed domain contrast is apparently connected with the monochromatic character of the applied LED illumination compared to the previously used continuous spectra of halogen or xenon lamps. The observation of magnetic domains by Kerr microscopy opens the door to study the local dynamics of the magnetization process in these multiferroic materials.

ACKNOWLEDGMENTS

O. Perevertov and O. Heczko were supported by the Czech Science Foundation under Project No. 15-00262S. We thank Kristyna Onderkova for sample preparation.

-
- [1] A. Hubert and R. Schäfer, *Magnetic Domains*, 3rd ed. (Springer, Berlin, 2008).
 - [2] W. K. Hiebert, A. Stankiewicz, and M. R. Freeman, *Phys. Rev. Lett.* **79**, 1134 (1997).
 - [3] T. Graf, C. Felser, and S. P. Parkin, *Prog. Solid State Chem.* **39**, 1 (2011).
 - [4] R. Kainuma, A. Cakir, C. Giacobbe, A. Al-Zubi, T. Hickel, M. Acet, and J. Neugebauer, *Nature (London)* **439**, 957 (2006).
 - [5] B. Dutta, A. Cakir, C. Giacobbe, A. Al-Zubi, T. Hickel, M. Acet, and J. Neugebauer, *Phys. Rev. Lett.* **116**, 025503 (2016).
 - [6] O. Heczko, A. Sozinov, and K. Ullakko, *IEEE Trans. Magn.* **36**, 3266 (2000).
 - [7] A. Sozinov, A. A. Likhachev, N. Lanska, and K. Ullakko, *Appl. Phys. Lett.* **80**, 1746 (2002).
 - [8] A. Sozinov, N. Lanska, A. Soroka, and W. Zou, *Appl. Phys. Lett.* **102**, 021902 (2013).
 - [9] A. Planes, L. Mañosa, and M. Acet, *J. Phys.: Condens. Matter* **21**, 233201 (2009).
 - [10] L. Straka, O. Heczko, H. Seiner, N. Lanska, J. Drahoš, A. Soroka, S. Fähler, H. Hänninen, and A. Sozinov, *Acta Mater.* **59**, 7450 (2011).
 - [11] H. H. Liebermann and C. D. Graham, *Acta Metallurgica* **25**, 715 (1977).
 - [12] Y. Ge, O. Heczko, O. Söderberg, and S.-P. Hannula, *Scr. Mater.* **54**, 2155 (2006).
 - [13] O. Heczko, K. Jurek, and K. Ullakko, *J. Magn. Magn. Mater.* **226**, 996 (2001).
 - [14] V. Kopecký, L. Fekete, O. Perevertov, and O. Heczko, *AIP Adv.* **6**, 056208 (2016).

- [15] Y. Ge, O. Heczko, O. Soderberg, and V. K. Lindroos, *J. Appl. Phys.* **96**, 2159 (2004).
- [16] M. De Graef, Y. Kishi, Y. Zhu, and M. Wuttig, *J. Phys. IV Proc.* **112**, 993 (2003).
- [17] V. C. Solomon, M. R. McCartney, and D. J. Smith, *Appl. Phys. Lett.* **86**, 192503 (2005).
- [18] H. D. Chopra, C. Ji, and V. V. Kokorin, *Phys. Rev. B* **61**, R14913 (2000).
- [19] A. Neudert, Y. W. Lai, R. Schäfer, M. Kustov, L. Schultz, and J. McCord, *Adv. Eng. Mater.* **14**, 601 (2012).
- [20] O. Perevertov and R. Schäfer, *Mater. Res. Express* **3**, 096103 (2016).
- [21] O. Perevertov and R. Schäfer, *J. Phys. D: Appl. Phys.* **47**, 185001 (2014).
- [22] K. Buschow, *Handbook of Magnetic Materials* (Elsevier, 1988), Vol. 4, p. 493.
- [23] L. Beran, P. Cejpek, M. Kulda, R. Antos, V. Holy, M. Veis, L. Straka, and O. Heczko, *J. App. Phys.* **117**, 17A919 (2015).
- [24] See Supplemental Material at <http://link.aps.org/supplemental/10.1103/PhysRevB.95.144431> for videos showing magnetic domains during the magnetization process for single- and multivariant states.
- [25] Y. W. Lai, R. Schäfer, L. Schultz, and J. McCord, *Appl. Phys. Lett.* **96**, 022507 (2010).